Surface Plasmon Resonance-like integrated sensor at terahertz frequencies for gaseous analytes.

Alireza Hassani and Maksim Skorobogatiy
maksim.skorobogatiy@polymtl.ca

www.photonics.phys.polymtl.ca

Engineering Physics Department.,École Polytechnique de Montréal, C.P. 6079, succ. Centre-Ville Montreal, Québec H3C3A7, Canada

Abstract: Plasmon-like excitation at the interface between fully polymeric fiber sensor and gaseous analyte is demonstrated theoretically in terahertz regime. Such plasmonic excitation occurs on top of a $\sim 30\mu m$ ferroelectric PVDF layer wrapped around a subwavelength porous polymer fiber. In a view of designing a fiber-based sensor of analyte refractive index, phase matching of a plasmon-like mode with the fundamental core guided mode of a low loss porous fiber is then demonstrated for the challenging case of a gaseous analyte. We then demonstrate the possibility of designing high sensitivity sensors with amplitude resolution of $3.4 \cdot 10^{-4}$ RIU, and spectral resolution of $1.3 \cdot 10^{-4}$ RIU in THz regime. Finally, novel sensing methodology based on detection of changes in the core mode dispersion is proposed.

OCIS codes: (130.6010) Sensors; (240.6680) Surface plasmons; (060.2370) Fiber optic sensors; (040.2235) Far infrared or terahertz; (060.5295) Photonic crystal fibers.

References and links

1. V. M. Agranovich and D. L. Mills, S*urface Polaritons - Electromagnetic Waves at Surfaces and Interfaces* (North-Holland, Amsterdam, 1982).
2. J. Homola, "Optical fiber sensor based on surface plasmon resonance excitation," Sens. Actuators B **29**, 401-405 (1995).
3. A. Hassani and M. Skorobogatiy, "Design criteria for the Microstructured Optical Fiber-based Surface Plasmon Resonance sensors," J. Opt. Soc. Am. B **24**, 1423-1429 (2007).
4. M. Skorobogatiy and A. V. Kabashin, "Photon Crystal waveguide-based surface plasmon resonance bio-sensor," Appl. Phys. Lett. **89**, 143518-143521 (2006).
5. B. Gauvreau, A. Hassani, M. F. Fehri, A. Kabashin, and M. A. Skorobogatiy, "Photonic bandgap fiber-based Surface Plasmon Resonance sensors," Opt. Express **15**, 11413-11426 (2007).
6. D. Wu, N. Fang, C. Sun and X. Zhang, "Terahertz plasmonic high pass filter," Appl. Phys. Lett. **83**, 201-203 (2003).
7. M. Qiu, "Photonic band structures for surface waves on structured metal surfaces," Opt. Express **13**, 7583-7588 (2005).
8. J.F. O'Hara and R. D. Averitt, "Prism coupling to terahertz surface plasmon polaritons," Opt. Express **13**, 6117-6126 (2005).
9. K. Wang and D. M. Mittleman, "Dispersion of Surface Plasmon Polaritons on Metal Wires in the Terahertz Frequency Range," Phys. Rev. Lett. **96**, 157401-147404 (2006).
10. Y. Chen, Z. Song, Y. Li, M. Hu, Q. Xing, Z. Zhang, L. Chai, and C. Y. Wang, "Effective surface plasmon polaritons on the metal wire with arrays of subwavelength grooves," Opt. Express **14**, 13021-13029 (2006).

#99949 - $15.00 USD Received 8 Aug 2008; revised 12 Nov 2008; accepted 13 Nov 2008; published 24 Nov 2008

11. J. G. Rivas, M. Kuttge, H. Kurz, P. H. Bolivar, and J. A. Snchez-Gil "Low-frequency active surface plasmon optics on semiconductors," Appl. Phys. Lett. **88**, 082106-082109 (2006).
12. J. W. Lee, M. A. Seo, D. J. Park, D. S. Kim, S. C. Jeoung, Ch. Lienau, Q. H. Park, and P. C. M. Planken, "Shape resonance omni-directional terahertz filters with near-unity transmittance," Opt. Express **14**, 1253-1259 (2006).
13. S. A. Maier, S. R. Andrews, L. Martin-Moreno, and F. J. Garcia-Vidal, "Terahertz Surface Plasmon-Polariton Propagation and Focusing on Periodically Corrugated Metal Wires," Phys. Rev. Lett. **97**, 176805-176807 (2006).
14. F. Miyamaru, M. W. Takeda, T. Suzuki, and C. Otani, "Highly sensitive surface plasmon terahertz imaging with planar plasmonic crystals," Opt. Express **15**, 14804-14809 (2007).
15. J. B. Pendry, A. J. Holden, W. J. Stewart, and I. Youngs, "Extremely Low Frequency Plasmons in Metallic Mesostructures," Phys. Rev. Lett. **76**, 4773-4776 (1996).
16. J. B. Pendry, A. J. Holdenz, D. J. Robbinsz, and W. J. Stewartz, "Low frequency plasmons in thin-wire structures," J. Phys.: Condens. Matter **10**, 4785-4809 (1998).
17. T. Hidaka, H. Minamide, H. Ito, J. Nishizawa, K. Tamura, and S.Ichikawa, "Ferroelectric PVDF Cladding Terahertz Waveguide," J. Lightwave Technol. **23**, 2469-2475 (2005).
18. Y. S. Jin, G. J. Kim, and S. G. Jeon, "Terahertz dielectric properties of polymers," J. Korean Phys. Soc. **49**, 513-517 (2006).
19. M. Skorobogatiy, A. Dupuis, A. Hassani, and N. Guo, "Designs of porous polymer THz fibers," Proceedings SPIE **6892**, 51 (2008).
20. A. Hassani, A. Dupuis, and M. Skorobogatiy, "Low Loss Porous Terahertz Fibers Containing Multiple Subwavelength Holes," Appl. Phys. Lett. **92**, 071101 (2008).
21. A. Hassani, A. Dupuis, and M. Skorobogatiy, "Porous polymer fibers for low-loss Terahertz guiding," Opt. Express **16**, 6340-6351 (2008).
22. T. D. Engeness, M. Ibanescu, S. G. Johnson, O. Weisberg, M. Skorobogatiy, S. Jacobs, and Y. Fink, "Dispersion tailoring and compensation by modal interactions in OmniGuide fibers," Opt. Express **11**, pp. 1175-1198, (2003)
23. B. T. Kuhlmey, K. Pathmanandavel, and R. C. McPhedran, "Multipole analysis of photonic crystal fibers with coated inclusions," Opt. Express **14**, pp. 10851-64, (2006)
24. S. A. Harmon and R. A. Chevillea, "Part-per-million gas detection from long-baseline THz spectroscopy," Appl. Phys. Lett. **85**, 2128-2130, (2004)
25. D. M. Mittleman, R. H. Jacobsen, R. Neelamani, R. G. Baraniuk, and M. C. Nuss,"Gas sensing using terahertz time-domain spectroscopy," Appl. Phys. B **67**, 379390, (1998)
26. R. Guo, K. Akiyama, H. Minamide, and H. Ito, "Frequency-agile terahertz-wave spectrometer for high-resolution gas sensing," Appl. Phys. Lett. **90**, 121127-9, (2007)

1. Introduction

In the visible and ultraviolet range, the collective oscillation of free charge carriers at a metal-dielectric interface yields a surface plasmon wave propagating along the surface of the metal [1, 2, 3, 4, 5]. Propagating at the metal/dielectric interface, surface plasmons are extremely sensitive to changes in the refractive index of the dielectric. This feature constitutes the core of many Surface Plasmon Resonance (SPR) sensors. Typically, in the visible range, these sensors are implemented in the Kretschmann-Raether prism geometry where p-polarized light is launched through a glass prism and reflected from a thin metal (Au, Ag) film deposited on the prism facet. The presence of a prism allows phase matching of an incident electromagnetic wave with a plasmonic wave at the metal/ambient dielectric interface at a specific combination of the angle of incidence and wavelength. Mathematically, phase matching condition is expressed as equality between the plasmon wave-vector and a projection of the wavevector of an incident wave along the interface [1].

The sensitivity of plasmon excitation to changes in the refractive index of the dielectric medium has been widely exploited for sensing applications. The plasma frequency, which imposes a lower frequency limit for the existence of these plasmons, is defined by $\omega_p^2 = ne^2/\varepsilon_0 m_e$, where n, e, ε_0, m_e are the electron density, electric charge, vacuum permittivity and electron mass. Since the free electron density in metals is typically in the range of 10^{22} cm^{-1}, the plasma frequency is frequently limited to the visible and ultraviolet regions. At frequencies significantly below the plasma frequency (like the THz range), large negative permittivity strongly prohibits electromagnetic fields from penetration inside a metal, and plasmon excitation on the metal/dielectric interface becomes challenging. Therefore, efficient

#99949 - $15.00 USD Received 8 Aug 2008; revised 12 Nov 2008; accepted 13 Nov 2008; published 24 Nov 2008

plasmonic excitation at lower frequencies requires materials with lower plasma frequencies [6, 7, 8, 9, 10, 11, 12, 13, 14, 15, 16]. Pendry et al. have suggested an artificial material in the form of a 2D subwavelength metallic wire lattice for which the effective plasma frequency is designable and equals $\omega_p^2 = 2\pi c^2/a^2 \ln(a/r)$ [15, 16]. Since this plasmon frequency relies on the wire radius, r, and the lattice constant, a, the geometrical parameters of the artificial structure can tune the electron plasma frequency of metal to the THz or sub-THz frequency range. Moreover, further studies have recently confirmed that artificial subwavelength-sized metal structures can tune the plasma frequency of metals to GHz or THz frequency range and allow metals to support plasmon-like surface waves at frequencies much lower than the visible range [6, 7, 10, 13].

Thanks to the refractive index behavior of the ferroelectric Polyvinylidene fluoride (PVDF) layer we demonstrate new type of plasmonic-like excitations in THz regime which was impossible before while using metal layers in THz regime. PVDF is a ferroelectric semi-crystalline polymer with a small absolute value of permittivity in the visible and near-IR regions. However, in the THz region the dielectric function of ferroelectric PVDF exhibits a resonance:

$$\varepsilon_{PVDF}(\omega) = \varepsilon_{opt} + \frac{(\varepsilon_{dc} - \varepsilon_{opt})\omega_{TO}^2}{\omega_{TO}^2 - \omega^2 + i\gamma\omega}, \tag{1}$$

where, according to [17] $\varepsilon_{opt} = 2.0$, $\varepsilon_{dc} = 50.0$, $\omega_{TO} = 0.3\,THz$, and $\gamma = 0.1\,THz$. Fig. 1 shows the real and imaginary parts of the refractive index of ferroelectric PVDF in the wavelength range between 100 μm (3 THz) and 700 μm (0.43 THz). The real part of the refractive index of PVDF in this region is less than one, while the imaginary part is positive and mostly larger than one. Therefore, the real part of the PVDF dielectric constant is negative and by analogy with the behavior of the metals in the visible range, PVDF layer is expected to support a plasmon-like excitation. Moreover, PVDF gives an opportunity to design a fully polymeric structure for THz plasmonic devices using such established mass production techniques as micro-embossing and fiber drawing, which potentially makes the fabrication process highly suitable for the industrial scale-up.

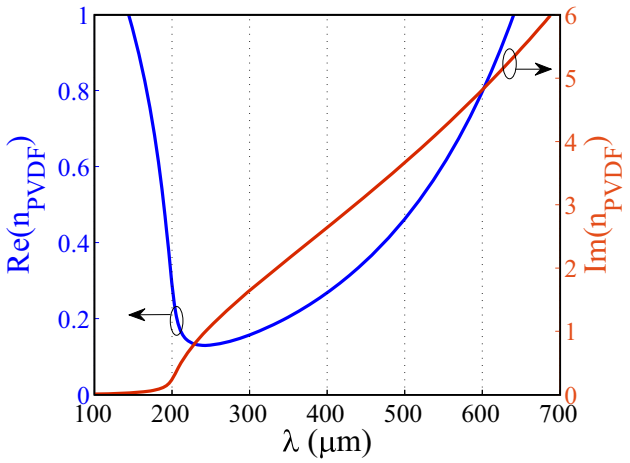

Fig. 1. The real and imaginary parts of the refractive index of ferroelectric PVDF.

This paper pursues two goals. The first goal is to show that thin layers of ferroelectric PVDF in air can support THz plasmon-like excitations similar to the ones found at the metal/dielectric interfaces in the visible range. The second goal is to design a fully polymeric integrated fiber-

#99949 - $15.00 USD Received 8 Aug 2008; revised 12 Nov 2008; accepted 13 Nov 2008; published 24 Nov 2008

based sensor in THz regime capable of detecting the index change in gaseous analytes (the most challenging case).

In direct analogy to SPR sensing in the visible, existence of plasmon-like resonances in THZ can enable study of the micron-sized particle binding dynamics within 10-60 μm of the sensor surface. This can be of particular interest for the label-free detection of specific bacteria by fictionalizing the sensor surface with bacteria specific phages. In comparison, SPR sensors in the visible can only detect binding of nano-molecules with sizes less than 100nm (size of a plasmon tail), rendering the method insensitive to the larger particles, such as bacteria.

It is worth mentioning that SPR sensing mechanism is completely different in spirit from spectroscopy based sensing. Particularly, plasmon-based sensors are mostly sensitive to changes in the real part of the refractive index in a thin sensing layer in the near vicinity of a metal surface. Specificity of a SPR sensor is achieved by coating a metal layer with a thin sensing layer that changes its refractive index when exposed to the target analyte. In contrast, spectroscopy based methods use detection of absorption lines in the spectrum of a target analyte, thus relying on existence of a spectroscopic "finger print" [24, 25, 26] for the detection and differentiation of a target. Moreover, when target analyte is weakly absorbing (which is, for example, the case for gas detection) one typically needs a several meter long gas cell to be able to measure absorption spectrum reliably. In a strike contrast to spectroscopic detection, SPR-based sensors can achieve the same sensitivity for low absorbing analytes in devices of only a few centimeters of length.

2. THz plasmon-like excitation at the PVDF/air interface

We start by explaining general ideas behind the principles of operation of a fiber-based SPR sensor. A typical configuration of such a sensor is a fiber with a thin metal layer deposited on its surface in the near proximity of a fiber core. Another side of a metal layer is facing the analyte to be monitored. During operation of a sensor, one launches a broadband light into the fiber core. In the vicinity of a specific wavelength defined by the sensor design, one of the core modes is phase matched (avoiding crossing of the corresponding dispersion relations) with a plasmon excitation mode confined to the metal/analyte interface. In the vicinity of such a resonant wavelength one observes dramatic decrease in the power transmitted through the fiber due to partial energy transfer from the core guided mode into a lossy plasmon wave. As dispersion relation of a plasmon mode is very sensitive to the refractive index of the analyte, resonant wavelength, and hence, spectral position of the absorption peak will shift when analyte refractive index is changed. By detecting spectral shift in the absorption peak of a core guided mode, changes in the analyte refractive index on the order of $10^{-4} - 10^{-5}$ RIU (Refractive Index Units) can be detected.

Based on the theory governing plasmon surface waves, effective refractive index of a plasmon excitation is typically close, while somewhat higher, than that of the analyte. On the other hand, effective refractive index of a fiber mode guided in a solid core is close to that of the core material. As there are no readily available optical materials that have refractive indices near 1, in practice, it becomes challenging to achieve phase matching between the plasmon and core guided modes when working with gaseous analytes. One solution [4, 5] that we have proposed to resolve the phase matching problem in the visible range was to use photonic bandgap fibers to design the effective refractive index of a core guided mode to be low enough so that phase matching with a plasmon becomes possible. The key advantage of using the photonic bandgap fibers is that fundamental core guided mode in such fibers can be, in principle, designed to have arbitrarily small effective refractive index. In practice, we have realized that photonic bandgap fibers that support Gaussian-like core mode with too low of an effective refractive index, necessarily have very small core sizes, thus leading to coupling challenges.

#99949 - $15.00 USD Received 8 Aug 2008; revised 12 Nov 2008; accepted 13 Nov 2008; published 24 Nov 2008

An alternative solution to the phase matching problem is to greatly lower the effective refractive index of a core guided mode by making the material of a fiber core highly porous (with the pore sizes being sub-wavelength). Such approach in THz regime has an additional advantage of low loss guidance outside of a phase matching point with a plasmon, as effective material absorption is greatly reduced in porous materials. As a particular design for such a fiber we consider a Teflon rod of 1480 μm diameter having porous core in the form of 4 layers of hexagonally arranged subwavelength holes. In the following simulations the hole-to-hole distance (the pitch) is considered to be 86 μm, while the hole diameter is 76 μm. The refractive indices of Teflon and air are taken to be 1.59 and 1.0 respectively. From outside, the teflon rod is covered with a thin PVDF layer facing air. In the following simulations we consider two thicknesses of a PVDF layer - 30 μm and 35 μm. Sub-wavelength single mode porous fibers for THz have been first introduced in [19, 20, 21], and they were demonstrated to support Gaussian-like fundamental mode with effective refractive index close to 1, while being also resistent to bending losses even for tight bending radii.

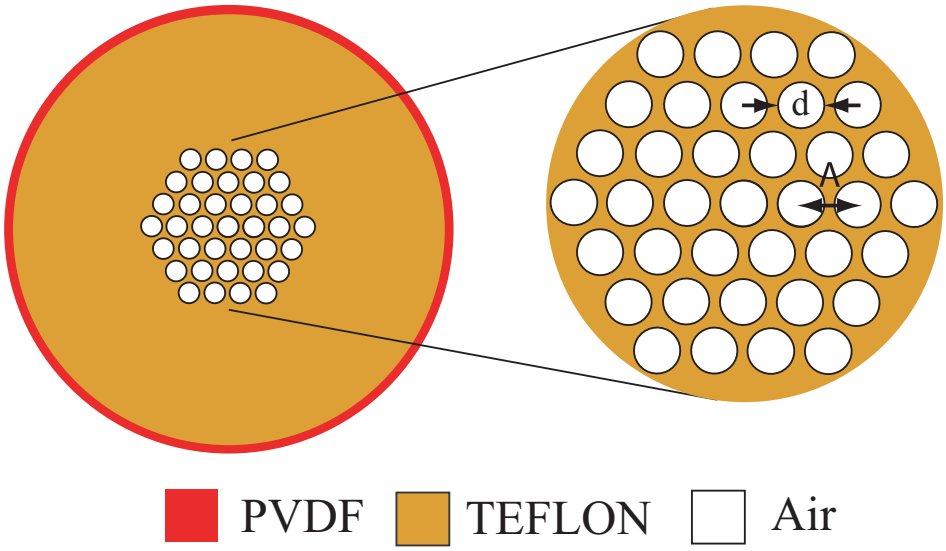

Fig. 2. Schematic of a porous THz fiber with a PVDF layer facing analyte.

As detailed in [19, 20, 21], introduction of sub-wavelength holes in the fiber core allows to lower dramatically the effective refractive index of the core guided mode. This, in turn, makes phase matching possible between the core guided mode and THz plasmon propagating at the PVDF/air interface. Furthermore, outside of the phase matching point, most energy in the Gaussian-like core mode is guided in the subwavelength holes, thus resulting in greatly reduced absorption loss. In Fig. 3 we present dispersion relation and losses of a core guided and plasmonic modes for a structure defined in Fig. 2. Particularly, Fig. 3(a) presents the effective refractive index of the core guided and plasmon modes as a function of wavelength for the two values of a PVDF thickness. Avoided mode crossing between the two modes around the wavelength of 300 μm is clearly visible. In Fig. 3 (b), losses of the core guided and plasmonic modes near the point of avoided crossing are shown. Losses of a core guided mode peak ($\sim$ 30dB/cm) at the point of phase matching with a plasmon, while being much lower (¡10dB/cm)) outside of the phase matching region (see also Fig. 6). In order to highlight increase in core mode losses solely due to its coupling to a plasmon, in our simulations we consider that Teflon material is lossless. In fact, bulk Teflon loss is reported to be $\sim$1.3dB/cm. When added to

#99949 - $15.00 USD Received 8 Aug 2008; revised 12 Nov 2008; accepted 13 Nov 2008; published 24 Nov 2008

simulations we find that Teflon material loss increases the loss of a core guided mode by mere 0.2dB/cm in the vicinity of 300 μm. Clearly, loss contribution due to bulk material loss of Teflon is much smaller than loss contribution due to coupling to a plasmon (absorption in a PVDF layer), even outside of a phase matching point.

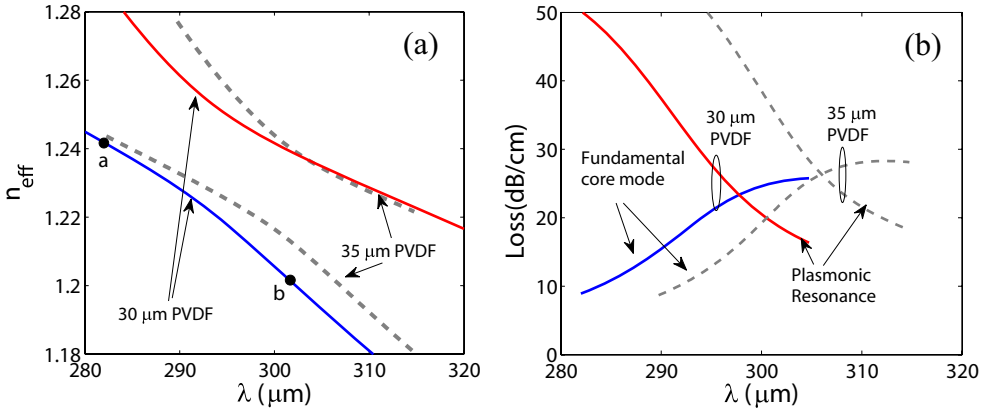

Fig. 3. Avoided crossing of the dispersion relations of the fundamental core mode and a THz plasmon-like excitation in a porous fiber with PVDF layer. The figure shows the a) real, and b) imaginary parts of the refractive index of the two modes as a function of wavelength.

In Fig. 4 we present distribution across the fiber crossection of the longitudinal energy flux component Sz for a core guided mode in the vicinity of a phase matching point. Only 1/4 of the fiber crossection is shown due to symmetry. Figures 4(a),(b), correspond to the points (a) and (b) on the core mode dispersion curve in Fig. 3(a). As expected, near the phase matching point core mode (high flux intensity in the air holes in the porous core) is strongly hybridized with a plasmon (high flux intensity at the PVDF/air interface).

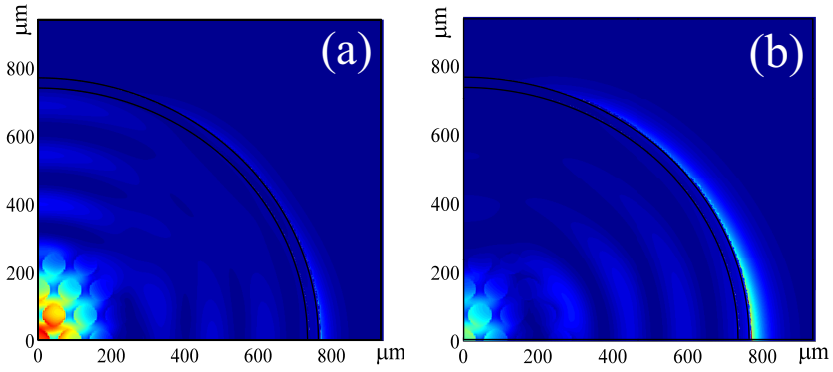

Fig. 4. Longitudinal energy flux component distribution across the fiber crossection for the core guided mode in the vicinity of a phase matching point with a plasmon. Plots (a) and (b) are calculated for the points (a) and (b) in Fig. 3a).

In Fig. 5 we also present dispersion of a core guided mode versus wavelength in the vicinity of a phase matching point. Two solid curves in Fig. 5 correspond to the two values of the

#99949 - $15.00 USD Received 8 Aug 2008; revised 12 Nov 2008; accepted 13 Nov 2008; published 24 Nov 2008

air refractive index $n_a = 1$ and $n_a = 1.01$ (only the refractive index of air outside the fiber is varied), assuming PVDF layer thickness of 30 μm. All the dispersion curves show a positive peak at the phase matching point, while passing through zero and becoming negative outside of the phase matching region. Note that even a small change in the air refractive index changes considerably dispersion of a core guided mode near the phase matching point. Thus, a 1% increase in the air refractive index shifts the dispersion peak by about 2 μm, while reducing mode dispersion by about 20 ps/nm-km (from about 35 ps/nm-km). Such strong changes are related to the sensitivity of a plasmon mode dispersion relation to the changes in the refractive index of air at the PVDF/air interface. Furthermore, the dispersion of fiber core mode is very sensitive to the PVDF layer thickness. Particularly, dashed line in Fig. 5 is computed using $n_a = 1$, and PVDF layer thickness of 35 μm. One observes that the dispersion peak shifts about 4 μm and increases by almost 50 ps/nm-km when the thickness of a PVDF layer increases from 30 to 35 μm.

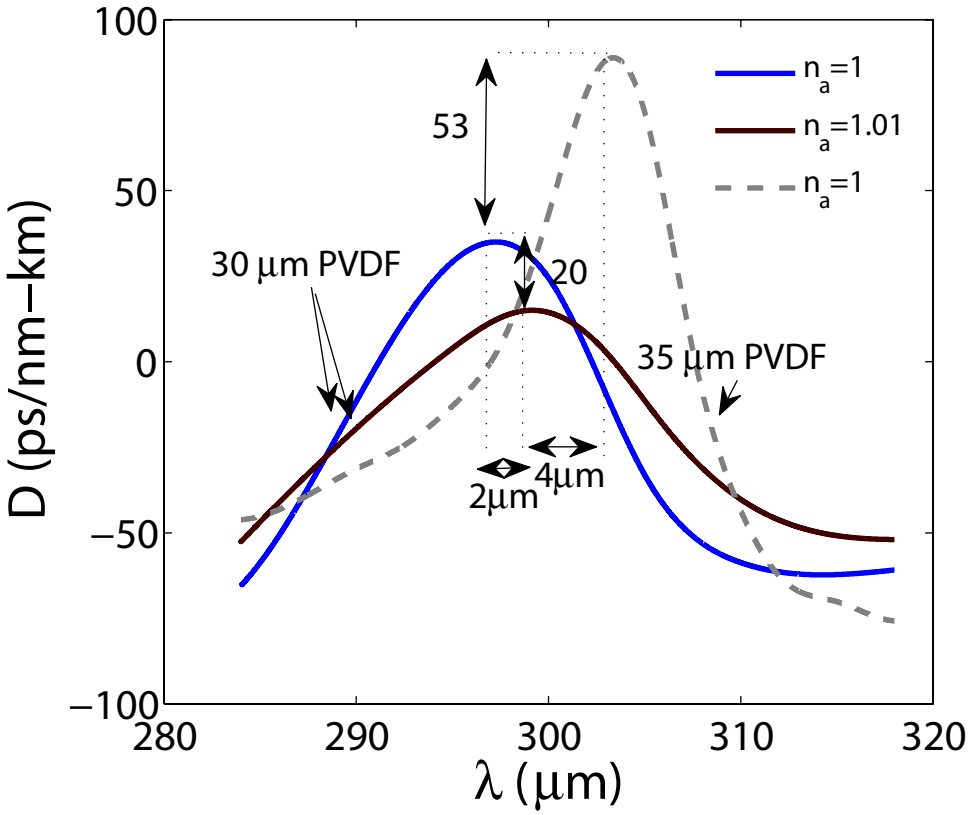

Fig. 5. Dispersion of the core guided mode of a porous core fiber covered with a thin PVDF layer facing air analyte (see Fig. 2). Solid curves - PVDF layer thickness 30 μm, two different values of the air analyte refractive index $n_a = 1$, $n_a = 1.01$. Dashed curve - PVDF layer thickness 35 μm, $n_a = 1$.

#99949 - $15.00 USD Received 8 Aug 2008; revised 12 Nov 2008; accepted 13 Nov 2008; published 24 Nov 2008

3. Sensitivity of an SPR-like THz sensor

Here, we address the question of sensitivity of a proposed SPR-like sensor to the changes in the refractive index of analyte. One mode of operation of a proposed sensor is by registering at a fixed frequency the changes in the amplitude of a transmitted light. We define $\alpha(\lambda, n_a)$ to be the transmission loss of the fiber core mode as a function of the wavelength and the refractive index of analyte n_a. Considering P_0 to be the power launched into the fiber core mode, the power detected after propagation along the sensor of length L will be $P(L,\lambda,n_a) = P_0 \exp(-\alpha(\lambda,n_a)L)$. For the operational wavelength λ, the amplitude sensitivity to the dn_a change in the analyte refractive index can then be defined as:

$$S_A(\lambda)[RIU^{-1}] = \frac{1}{P(L,\lambda,n_a)} \frac{P(L,\lambda,n_a+dn_a) - P(L,\lambda,n_a)}{dn_a}. \quad (2)$$

The sensor length L is typically limited by the modal transmission loss. A reasonable choice of a sensor length is $L = 1/\alpha(\lambda,n_a)$; such a choice of sensor length results in a simple definition of sensitivity with respect to small changes in the analyte refractive index:

$$S_A(\lambda)[RIU^{-1}] = \frac{1}{P(L,\lambda,n_a)} \frac{\partial P(L,\lambda,n_a)}{\partial n_a} = -\frac{1}{\alpha(\lambda,n_a)} \frac{\partial \alpha(\lambda,n_a)}{\partial n_a}. \quad (3)$$

In Fig. 6 we present amplitude sensitivity of the porous-core fiber-based Surface Plasmon Resonance (SPR) sensor as defined by Eq. (3). The maximal sensitivity is achieved at 292 μm and equals to 29 RIU^{-1}. Assuming that 1% change in the transmitted intensity can be reliably detected, sensor resolution of $3.4 \cdot 10^{-4}$ RIU is predicted.

Another way of defining sensor sensitivity is via a spectral measurement. Particularly, by detecting $\Delta\lambda_p$ shift in the position of a resonant absorption peak for Δn_a change in the refractive index of analyte one can define spectral sensitivity as $S_\lambda = \Delta\lambda_p/\Delta n_a$. For example, in Fig. 6 we show loss curves of a core guide mode calculated for the two different values of an air analyte refractive index $n_a = 1$ and $n_a = 1.01$. As seen from Fig. 6, analyte refractive index change of 0.01 results in a 4 μm shift of a loss peak, thus defining spectral sensitivity to be $S_\lambda = 400\mu m/RIU$. Assuming a typical 100MHz spectral resolution of a time domain THz setup (equivalently 30nm wavelength resolution at 1THz), sensor resolution of $1.3 \cdot 10^{-4}$ RIU is predicted.

4. Conclusion

In conclusion, fully polymeric SPR-like sensor is demonstrated in THz using porous core fiber covered with a thin feroellectric PVDF layer facing gaseous analyte. Plasmon-like excitation at the PVDF/air interface can be excited by the fiber core mode when phase matching is satisfied. Similarly to the optical SPR sensors, guided core mode exhibits a pronounced loss peak at the point of its phase matching with a plasmon-like mode. Moreover, core mode dispersion varies dramatically in the same phase matching region. By detecting changes in the wavelength of phase matching due to changes in the analyte refractive index, highly sensitive detection systems are possible. We show that both amplitude-based and spectral-based detection methods lead to sensitivities to the changes in the gaseous analyte refractive index on the order of $\sim 10^{-4} RIU$.

#99949 - $15.00 USD Received 8 Aug 2008; revised 12 Nov 2008; accepted 13 Nov 2008; published 24 Nov 2008

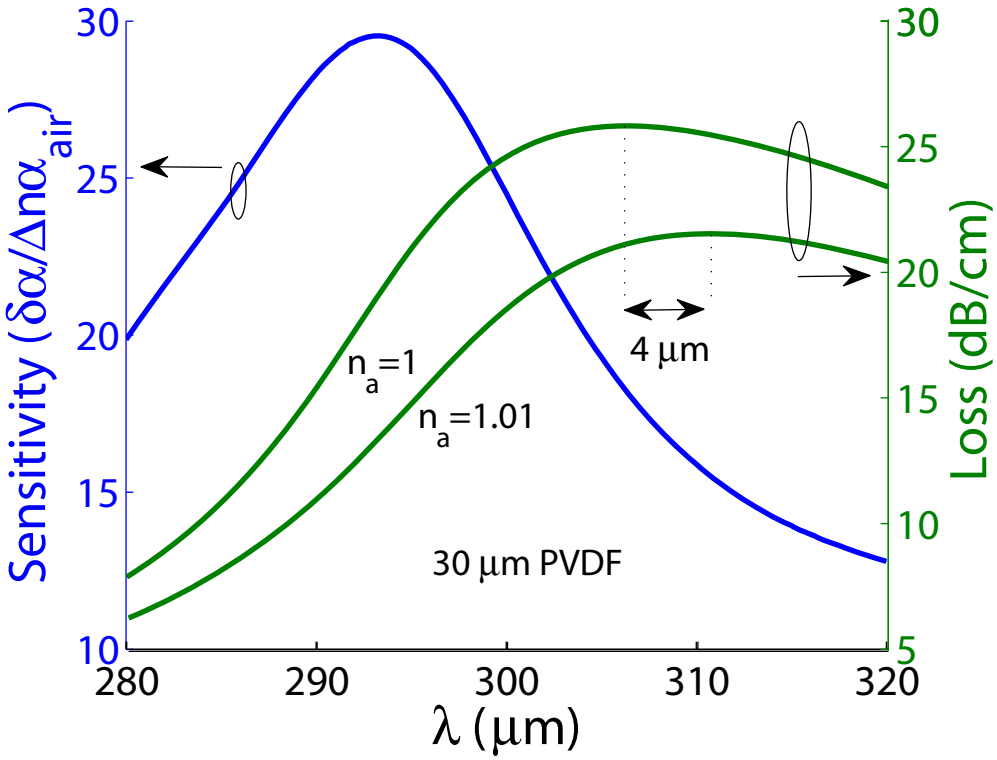

Fig. 6. Sensitivity of a porous-core fiber sensor featuring a 30 μm PVDF layer facing air analyte (blue line). Losses of a core guided mode versus wavelength (green lines) in the vicinity of a phase matching point with a plasmon for two values of the analyte refractive index $n_a = 1$, $n_a = 1.01$.

#99949 - $15.00 USD Received 8 Aug 2008; revised 12 Nov 2008; accepted 13 Nov 2008; published 24 Nov 2008